ANTIMICROBIAL AGENTS AND CHEMOTHERAPY, June 2011, p. 2576–2584 Vol. 55, No. 6
0066-4804/11/$12.00 doi:10.1128/AAC.01409-10

Artesunate Tolerance in Transgenic *Plasmodium falciparum* Parasites Overexpressing a Tryptophan-Rich Protein▽†

Guillaume Deplaine,[1,2,3]‡ Catherine Lavazec,[1,2,4,5]‡ Emmanuel Bischoff,[4,5] Onguma Natalang,[1,2]§ Sylvie Perrot,[1,2] Micheline Guillotte-Blisnick,[1,2] Jean-Yves Coppée,[6] Bruno Pradines,[7] Odile Mercereau-Puijalon,[1,2] and Peter H. David[1,2]*

Institut Pasteur, Unité d'Immunologie Moléculaire des Parasites, Département de Parasitologie Mycologie, F-75015 Paris, France[1]; CNRS, URA2581, F-75015 Paris, France[2]; INSERM-UPMC (Paris 6 University) UMRS 945, F-75013 Paris, France[3]; Institut Pasteur, Unité de Recherche Génétique et Génomique des Insectes Vecteurs, Département de Parasitologie Mycologie, F-75015 Paris, France[4]; CNRS Unit URA3012, Hosts, Vectors and Infectious Agents, F-75015 Paris, France[5]; Institut Pasteur, Plate-forme 2-Transcriptome et Epigénome, F-75015 Paris, France[6]; and Unité de Parasitologie, Unité Mixte de Recherche 6236, Institut de Recherche Biomédicale, des Armées–Antenne de Marseille, Marseille, France[7]

Received 13 October 2010/Returned for modification 26 December 2010/Accepted 15 March 2011

Due to their rapid, potent action on young and mature intraerythrocytic stages, artemisinin derivatives are central to drug combination therapies for *Plasmodium falciparum* malaria. However, the evidence for emerging parasite resistance/tolerance to artemisinins in southeast Asia is of great concern. A better understanding of artemisinin-related drug activity and resistance mechanisms is urgently needed. A recent transcriptome study of parasites exposed to artesunate led us to identify a series of genes with modified levels of expression in the presence of the drug. The gene presenting the largest mRNA level increase, *Pf10_0026* (*PArt*), encoding a hypothetical protein of unknown function, was chosen for further study. Immunodetection with PArt-specific sera showed that artesunate induced a dose-dependent increase of the protein level. Bioinformatic analysis showed that *PArt* belongs to a *Plasmodium*-specific gene family characterized by the presence of a tryptophan-rich domain with a novel hidden Markov model (HMM) profile. Gene disruption could not be achieved, suggesting an essential function. Transgenic parasites overexpressing PArt protein were generated and exhibited tolerance to a spike exposure to high doses of artesunate, with increased survival and reduced growth retardation compared to that of wild-type-treated controls. These data indicate the involvement of *PArt* in parasite defense mechanisms against artesunate. This is the first report of genetically manipulated parasites displaying a stable and reproducible decreased susceptibility to artesunate, providing new possibilities to investigate the parasite response to artemisinins.

Recent progress in the implementation of control measures, including bed nets and artemisinin combination therapy (ACT), has decreased the mortality/morbidity linked to *Plasmodium falciparum* malaria in several regions in which it is endemic (http://www.who.int/malaria/publications/atoz/9789241563697/en/index.html). However, malaria remains a major health problem for one-third of the world population. Increasing *Plasmodium falciparum* drug resistance is even more of a concern since emerging *in vitro* resistance to one of the major groups of drugs, artemisinins, has been observed (27, 39, 53). Moreover, treatment failures to recently introduced ACT are on the increase (15), which challenges the strategy of the containment of artemisinin-resistant malaria by the elimination of parasites using ACT (35). While the discovery of new drugs is an urgent need, an understanding of the artemisinins' mode of action and resistance mechanisms is a research priority.

Artesunate is a water-soluble artemisinin derivative. Artemisinins are endoperoxide-containing sesquiterpene lactones, and their mode of action remains controversial (13, 21). The Fe^{2+}-dependent activation of the endoperoxide bridge is required for the drug to be active (31, 33). The hypothesis that the cleavage of the endoperoxide moiety forms highly reactive oxyl radicals that rearrange to more stable carbon-centered radical intermediates, leading to covalent adducts with parasite products (2), has been disputed (24). While there is evidence to suggest the existence of a specific target, the *P. falciparum* SERCA-type Ca^{2+} pump (PfATPase6) (17), the ability of artemisinins to inhibit SERCA varies between studies (32). Artesunate also could act by protecting heme from polymerization, thus facilitating its transport to the food vacuole membrane, where it is able to exercise its cytotoxic activity (1). Finally, the mitochondrion has been characterized as a target (49). The formation of covalent adducts may be responsible for a pleiotropic effect of the drug on multiple targets and/or organelles.

In a study of the parasite transcriptome upon short exposure to lethal doses of artesunate, we showed that close to 400 genes presented modified transcript levels (37). Few genes were related to metabolic pathways, and most encoded chaperones, transporters, kinases, Zn-finger proteins, transcription-activat-

* Corresponding author. Mailing address: Institut Pasteur, Unité d'Immunologie Moléculaire des Parasites, Département de Parasitologie Mycologie, CNRS, URA2581, F-75015 Paris, France. Phone: 33 (0) 1 40 61 31 72. Fax: 33 (0) 1 42 73 22 40. E-mail: pdavid@pasteur.fr.

† Supplemental material for this article may be found at http://aac.asm.org/.

‡ These authors contributed equally.

§ Present address: Division of Genetics and Genomics, School of Biological Sciences, Nanyang Technological University, Singapore.

▽ Published ahead of print on 4 April 2011.

ing proteins, and proteins involved in proteasome degradation, oxidative stress, and cell cycle regulation. More than pointing to a defined target of the drug, these observations seemed to reflect the parasite response aimed at drug-induced injury repair, the path of events leading to parasite death, or a combination of both. More than half of the genes showing modified expression under artesunate pressure encoded hypothetical proteins with unknown functions, as could be expected from the existence of a high percentage of such genes in the *P. falciparum* genome. Among these, *Pf10_0026* (*PArt*) displayed the highest expression increase of all genes in response to the drug. *Pf10_*0026 has been annotated in the Plasmo DB (http://plasmodb.org/plasmo/) as a "tryptophan-rich antigen 3, putative" with unknown function. We sought to gain insight into its possible involvement in response to artemisinins. In particular, we sought to determine whether its overexpression reflected either a parasite response to overcome artesunate toxicity or more general perturbations on the path to cellular death.

We showed that the increase of *PArt* steady-state RNA actually resulted in a dose-dependent increase of the corresponding protein under artesunate pressure. Sequence analysis and genome mining showed that the *PArt* product belonged to a *Plasmodium*-specific protein family characterized by a novel HMM (hidden Markov model) profile with a conserved arrangement of tryptophan residues. Attempts to generate mutant parasites with a disrupted *PArt* gene were unsuccessful in culture, suggesting an essential role of *PArt* for *P. falciparum* development. Episome-driven overexpression bestowed on the resulting recombinant parasites the capacity to tolerate exposure to increased doses of artesunate. These data indicate that *PArt* modulates parasite sensitivity to the drug. This is the first report of genetically manipulated parasites displaying a stable and reproducible decreased susceptibility to artesunate.

MATERIALS AND METHODS

Ethics statement. Animal studies were carried out in strict accordance with the French (Décrets 87-848, R214-87 and R214-122 du Code rural) and European (86/609/CEE) regulations concerning the use of animals for biological research purposes. All efforts were made to minimize suffering. Authorization was approved by the French Direction Départementale des Services vétérinaires de Paris en Charge des Affaires Vétérinaires d'Ile de France (permit number 75-287 delivered 09/04/07).

Parasite culture and synchronization. The FCR3 strain (FUP/CB line) (18) of *P. falciparum* was used throughout the experiments. The FUP/CB strain and transgenic parasites were cultured under conditions derived from the method described by Trager and Jensen (48). Briefly, parasites were grown at 37°C in leukocyte-free human O^+ erythrocytes (5% hematocrit) in RPMI 1640 medium (Gibco Life Technologies) supplemented with 10% (vol/vol) AB^+ human serum, 25 mM HEPES (Sigma, St. Louis, MO), 200 mM hypoxanthine (Sigma), 0.2% $NaHCO_3$ (Sigma) under an atmosphere of 5% CO_2, 1% O_2, and 94% N_2. Cultures were synchronized successively by the concentration of mature schizonts using plasmagel flotation (42), followed 3 h after invasion by the alanine lysis of residual maturing forms (20).

Plasmid construction and parasite transformation. The FCR3 strain (FUP/CB line) was used to attempt parasite knockout as well as the overexpression of *PArt*.

Plasmids were constructed to disrupt the *PArt* gene using a single-crossover strategy with pHC1c vector (9) or a double-crossover strategy with pHTTK vector (16). The plasmid pHC1c/*PArt* was constructed by inserting a 1,000-bp PCR product of *PArt* from *P. falciparum* FUP/CB amplified using the following primers: PArt-HindIII-forward, ′ACAAGCTTGCAGTACATTTTTAAGAGGA; PArt-XhoI-reverse, 5′AACTCGAGGGGTATATTATTTTGTATCATTCC (underlining indicates the introduced restriction enzyme site). To perform the double-crossover strategy using pHTTK, a first insert was generated by DNA amplification using the following primers: insert1-SpeI-forward, 5′GGACTAGTACGATATTTGTATGAATTGG; insert1-BglII-reverse, 5′GGAGATCTTCCTCTTAAAAATGTACTGC. The second insert was generated with the following primers: insert2-ClaI-forward, 5′GGATCGATGTCACAAGCAAATGTAGTCG; insert2-*Nco*-reverse, 5′GGCCATGGTCAGATGTTGAATTGTTCCC. Overexpression was achieved using pHL-dhfr-3myc vector (34). This plasmid contains three consecutive c-myc epitopes within an expression cassette that is driven by the *P. falciparum* 5′ *hrp3* promoter and 3′ *hrp2* terminator, ensuring a high expression level of the *PArt* gene. A human dihydrofolate reductase (hDHFR) expression cassette allows the selection of transformed parasites with pyrimethamine. The full length of *PArt*, intron included, from *P. falciparum* FUP/CB genomic DNA was amplified using the following primers: XhoI-forward, 5′GGCTCGAGATGCAAATTAATCCAATGG; BamHI-reverse, 5′AAGGATCCTTCTTGGTTTCTAATTAATTCC.

The PCR product was restriction digested with XhoI and BglII and then inserted into the expression vector pHL-dhfr-3myc, leading to pHL-*PArt*-3myc. As a control for survival studies under artesunate pressure, we used the pHL-rif-3myc line harboring the myc tag in frame with *rif* gene *PFB1050w* in the same vector.

Knockout vectors and expression vectors were transfected into the FUP/CB line by preloading red blood cells (RBC) as described previously (11). Briefly, 300 μl of red blood cells was washed once with 5 ml of incomplete cytomix (52) and then combined with 100 μg of plasmid DNA to a total volume of 400 μl. The cells were transferred to a 0.2-cm cuvette, chilled on ice, and electroporated using a Bio-Rad Gene Pulser and conditions of 0.31 kV and 960 μF. DNA-loaded RBC then were washed with culture media. Mature stages were incubated with the DNA-loaded RBC. Transfection was achieved after reinvasion. Transformant parasites were selected 48 h after transfection by being cultured in medium containing 100 ng/ml pyrimethamine.

Drug treatment. Artesunate (Sanofi Aventis) was dissolved in 100% ethanol, and a 1-μg/μl (2.6 mM) stock solution was aliquoted and kept at −20°C. FUP/CB and mutant *PArt*/myc lines were exposed to 0, 20, 40, 60, 80, 100, 200, and 400 ng/ml of artesunate (52, 104, 156, 208, 260, 520, and 1,040 nM, respectively), at 2% hematocrit, for 3 h. Parasites then were washed three times at room temperature and cultured at 37°C. Subsequent parasite growth was assessed by the microscopic examination of Giemsa-stained thin blood smears prepared at 0 h (when drug was added) and at 3, 48, and 72 h after drug treatment.

A one-sided rank-sum Wilcoxon test was used to determine drug concentrations for which the survival rate of PArt/myc line was significantly increased compared to that of controls.

Chemosusceptibility profiles of FUP/CB and PArt/myc lines to artesunate and 8 other antimalarials were measured using a 42-h *in vitro* isotopic microtest. The drug concentrations able to inhibit 50% of parasite growth (IC_{50}) were determined using a 42-h microtest as described in reference 6. Briefly, 200 μl/well of a suspension of synchronous parasitized red blood cells was distributed in 96-well plates predosed with antimalarial drugs. Parasite growth was assessed by adding 1 μCi of tritiated hypoxanthine to each well at time zero. The plates then were incubated for 48 h. The radioactivity incorporated in nucleotides by the parasites was measured with a scintillation counter. The IC_{50} was designated the concentration at which the tritiated hypoxanthine incorporation reached 50% of the total incorporation by parasites in the drug-free control wells. The IC_{50} was determined by nonlinear regression analysis of log-based dose-response curves (Riasmart; Packard, Meriden, CT).

Mouse immunization. A group of six mice (outbred-OF1; female mice; 6 to 8 weeks old; Charles River, France) were immunized by subcutaneous injection at 3-week intervals with soluble recombinant PArt N- or C-terminal polypeptide (residues 1 to 569 and 664 to 979, respectively) produced in *Escherichia coli* (Proteogenix). Immunizations were carried out in the presence of Freund's adjuvant. Sera were collected before the first injection (preimmune sera) and 10 days after the third injection.

Antiserum raised against the C-terminal part of the molecule revealed a band migrating at about 118 kDa on Western blots (see Fig. 2) but not with the other three members of the *P. falciparum* tryptophan-rich family (predicted masses of 80.5, 34.5, and 94.5 kDa for PF08_0003, PFA0135w, and MAL13P1.269, respectively). In contrast, antisera raised against the N-terminal portion of PArt generated several bands on Western blots (data not shown). Such cross-reactivity probably was related to the multiple NNN repeats of the protein, a common occurrence in multiple *P. falciparum* protein, excluding this serum from further analysis.

Western blot analysis. Trophozoites were prepared from gel flotation, and pellets were washed three times in phosphate-buffered saline (PBS) and extracted in boiling Bio-Rad sample buffer containing reducing agent. After 10 min at 100°C, samples were immediately frozen at −80°C at a concentration of 5×10^6 parasites/10 μl (crude extract). The electrophoresis of samples using reduc-

ing 4 to 12% SDS-PAGE precast gels (Bio-Rad) was followed by transfer onto a polyvinylidene difluoride (PVDF) membrane. The membrane was blocked with 5% skim milk–PBS, pH 7.4, and probed at 37°C for 1 h with antibodies in PBS–5% skim milk–0.02% Tween 20. Mouse antiserum directed against the W-rich portion of a PArt recombinant protein was used at a 1:400 dilution, a rabbit anti-histone H3 (Abcam) antibody at a 1:1,000 dilution, a mouse monoclonal anti-myc antibody (Invitrogen) at a 1:5,000 dilution, and a mouse monoclonal anti-HSP70 antibody at a 1:500 dilution. After being washed, membranes were incubated for 1 h with horseradish peroxidase-conjugated anti-rabbit or anti-mouse IgG secondary antibody (Promega) at a 1:25,000 dilution in PBS–5% skim milk–0.02% Tween 20. A detection step was performed using the Pierce chemiluminescence system by following the manufacturer's instructions. Uninfected RBC crude extracts were used as controls and were processed similarly to washed RBCs. The levels of PArt were quantified by densitometry using Quantity One analysis software (Bio-Rad). For each band, the specific densitometry was determined by subtracting the area containing the band from an adjacent empty area. For each sample, we then calculated the ratio of protein levels for PArt/histone H3 and PArt/HSP70 and quantified the increase of PArt signal relative to that of the loading control under increasing doses of artesunate.

Immunofluorescence assay. Synchronized parasites harvested at different developmental stages were thinly smeared, air dried, and fixed for 20 min in methanol chilled at −80°C. Slides were blocked in 2% bovine serum albumin (BSA) in PBS and then incubated for 1 h with 1:100 dilutions of mouse immune serum against the W-rich C-terminal portion of PArt and/or rabbit immune serum directed against *P. falciparum* Rab6 (10) (kindly provided by G. Langlsey).

After three washes in PBS, slides were incubated for 1 h with Alexa Fluor 488-conjugated goat anti-mouse affinity-purified IgG and/or Alexa Fluor 594-conjugated goat anti-rabbit affinity-purified IgG (Molecular Probes). Parasite nuclei were stained with Hoechst 33342 (diluted 1:20,000; Molecular Probes). Slides were washed three times in PBS and mounted in Slowfade Gold antifade reagent (Invitrogen). Samples were examined under an epi-illumination microscope (DMI 6000; Leica) with a cooled charge-coupled device (CCD) camera (MicroMax; Princeton Instruments). Images were acquired with MetaMorph (Molecular Devices) and processed with MetaMorph and Photoshop CS2 (Adobe Systems, San Jose, CA).

HMM searches. Protein homologous sequences of PArt were collected by an NCBI-BLASTP search with a nonredundant protein sequence database. Twenty sequences were selected with a P value of $<10^6$ and aligned by MegAlign (Lasergene; DNASTAR), and an HMM profile was generated using hmmbuild (HMMER package; http://hmmer.org). Sequences were searched with hmmsearch from Uniprot or nrprot (NCBI), and 79 sequences matched the HMM profile. A final HMM profile was generated after the alignment of the sequences considered hits.

Reverse transcription and quantitative PCR (qPCR). Parasite cultures were harvested by centrifugation and lysed in 5 pellet volumes of Trizol (Gibco) before being frozen at −80°C. Total RNA was prepared from thawed samples by following the manufacturer's instructions. RNA quality was assessed with an Agilent 2100 Bioanalyzer.

RNA samples were treated with DNase I (Invitrogen) for 15 min at 37°C in the presence of RNAseOUT inhibitor (Invitrogen). RNA was reverse transcribed with Superscript II RT (Invitrogen) using random hexamers with a preextension step of 10 min at 25°C, followed by extension for 50 min at 42°C. cDNA then was treated with RNase H for 20 min at 37°C.

Quantitative real-time PCR was performed on cDNA using an ABI Prism 7900HT thermal cycler system (Applied Biosystems) for 40 cycles (95°C for 15 s, 55°C for 15 s, and 60°C for 45 s). Reactions were done in 20-μl volumes using SYBR green PCR master mix (Applied Biosystems) and 0.5 μM primers in triplicate with six concentrations of cDNA (2,500, 625, 156, 39, and 10 pg/μl) to assess primer amplification efficiency. The absence of DNA contamination was checked using RNA samples treated as cDNA without reverse transcriptase (2,500 pg/μl).

Transcript abundance was compared using the means of $\Delta\Delta C_T$ (threshold cycle) values calculated for all cDNA dilutions, with *PFI0425w* (putative transporter) as the endogenous normalizer. This gene was chosen because its expression level was not influenced by the presence of artesunate in all our experiments, and it showed very moderate levels of variation in whole-cycle transcriptome analysis (37). All experiments were realized with the following primers, which were designed using eprimer3: *PArt* 5′-forward, TTTAATTTTATCCTATTGT TTTGCCATATC; *PArt* 5′-reverse, TTTTTAAGCACAATATACATAAAGAG GGA; *PFI0425w* 5′-forward, AATACTACGAAAAAAATCGATGAATC; *PFI0425w* 5′-reverse, TCTTCACCTACAGGCTCTATATCAG.

A one-sided Wilcoxon rank-sum test was used to determine the drug concentration at which the expression ratio was significantly increased in the presence of the drug.

RESULTS

PArt is a tryptophan-rich (W-rich) protein that belongs to a *Plasmodium*-specific family. *In silico* analysis shows that *PArt* presents a two-exon gene structure encoding a protein with an estimated molecular mass of 118 kDa. A potential transmembrane domain was located within the first exon, but no export signal could be identified (Fig. 1A). Three-dimensional structure prediction suggested the existence of an amphiphilic alpha helix (GARNIER program; data not shown) similar to what was recently described for a *P. vivax* W-rich protein (4).

An NCBI-BLASTP search with a nonredundant protein sequence database identified 20 protein sequence homologues of PArt ($P < 10^6$). Among these protein sequences, a family of four *P. falciparum* tryptophan-rich proteins (PF08_0003, PFA0135w, MAL13P1.269, and PF10_0026 [*PArt*]) is characterized by a tryptophan-rich motif (40). The sequence alignment of 20 PArt homologues allowed the generation of a first HMM profile of the tryptophan-rich motif to which 79 sequences were found to match (see Table S1 in the supplemental material). A final HMM profile was generated after the alignment of the 79 sequences considered hits (Fig. 1B; also see Fig. S1 in the supplemental material). All 79 sequences were *Plasmodium* specific, as they were not found in any other genome, including those of apicomplexan parasites. Of these 79 genes, 35 paralogs were found in the genome of *P. vivax* (Pv-fam-a; e.g., PVX_096995). A very high degree of identity (96%) was found in the unique *PArt* orthologue of *P. reichenowi*, a simian parasite thought to be very closely related to *P. falciparum*.

Increase in *PArt* RNA levels upon exposure to artesunate results in increased protein expression. To determine whether an increase of *PArt* RNA under artesunate pressure, as demonstrated by transcriptomic studies, was reflected at the protein level, trophozoites were exposed to increasing doses of artesunate (from 10 to 400 ng/ml) for 3 h. A clear dose-dependent increase of the intensity of a band corresponding to a 118-kDa protein, PArt, was observed on Western blots and was revealed with an antiserum raised against the W-rich portion of the PArt recombinant protein (see Fig. S2 in the supplemental material). This increase began at exposure to 40 ng/ml of artesunate for 3 h, reaching 5- to 6-fold at 400 ng/ml in two separate experiments for which different reference proteins were used (histone H3 and PfHSP70; Fig. 2A and B, respectively). In parallel, real-time reverse transcription-PCR (RT-PCR) performed under increasing drug pressure showed significantly increased RNA levels beginning after 3 h of exposure to 80 ng/ml of artesunate, reaching a 3.4-fold increase at 400 ng/ml (Fig. 2C).

PArt is refractory to disruption in *P. falciparum* asexual blood stages. Bioinformatic analysis provided little evidence concerning the possible function of PArt. We attempted gene inactivation but were repeatedly unsuccessful in disrupting *PArt* (8 transfections with pHC1c/*PArt* and 10 with pHTTK/*PArt* were attempted without success). Both single- and double-crossover strategies led to effective transfection, as reflected by the emergence of drug-resistant parasites after 3

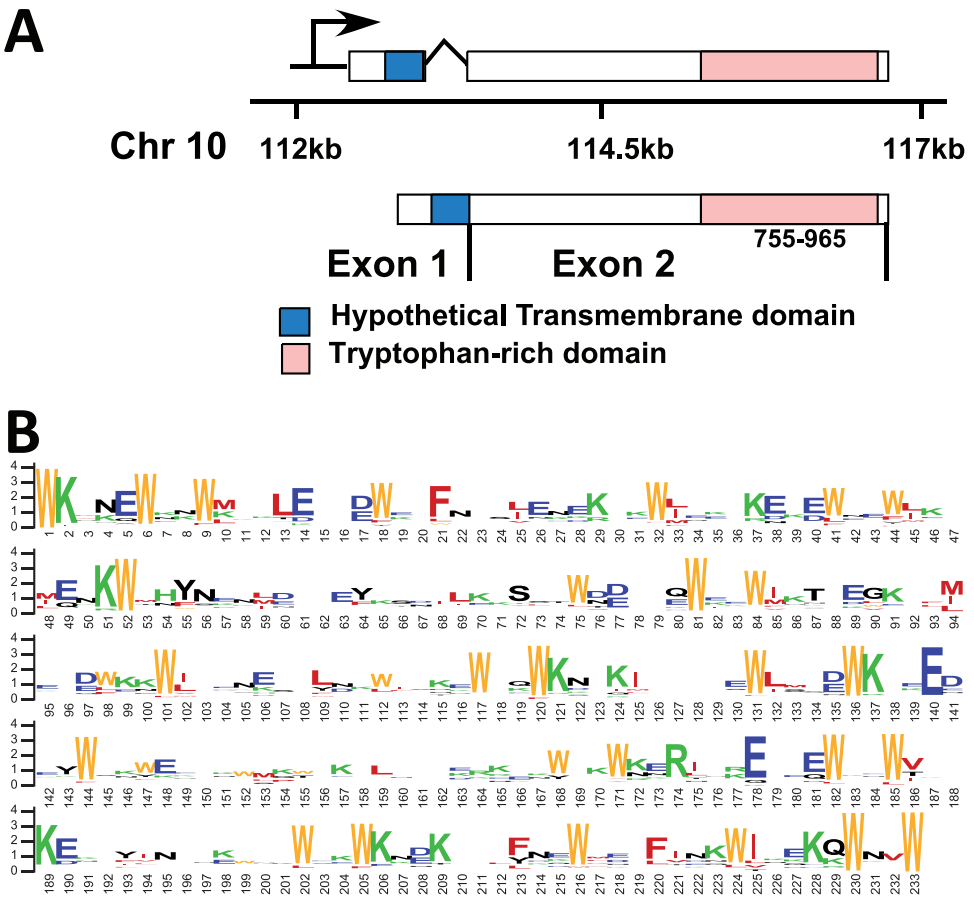

FIG. 1. Structure of *Pf10_0026* gene and tryptophan-rich domain. (A) Two-exon structure and localization of *Pf10_0026* on chromosome 10. The transmembrane domain is encoded at the 5′ end of exon 1 and the tryptophan-rich (W-rich) domain by the 3′ region of exon 2. The region corresponding to the W-rich domain encoded by residues 755 to 965 is shown on the mRNA structure. (B) HMM profile based on 79 genomic sequences of *Plasmodium* species showing a tryptophan-rich motif. The frequency of each amino acid is represented by the size of the amino acid one-letter code.

weeks of 100 ng/ml pyrimethamine or 4 ng/ml WR99210 treatment and by the PCR detection of the hDHFR-encoding sequence. However, Southern blot analysis showed that the hDHFR sequence was not integrated in the *PArt* locus (data not shown). Although not conclusive, these failed attempts are in favor of the essential character of *PArt* for the parasite erythrocytic cycle, at least *in vitro*.

Parasites overexpressing *PArt* show reduced susceptibility to artesunate. An overexpression strategy was adopted with the episomal expression of a myc-tagged gene driven by an *hrp3* promoter (34). A PArt/myc transfectant was obtained in which high levels (16-fold) of overexpression were achieved (Fig. 3A). RNA overexpression occurred mostly during the first 24 h of parasite development (Fig. 3B).

Indirect immunofluorescence showed a punctate distribution of PArt within the parasite cytoplasm on fixed trophozoite-infected RBC, with a marked fluorescence intensity increase in the PArt/myc-overexpressing line (Fig. 4A and B). There was no significant overlap with the Golgi apparatus, which was visible upon labeling with a rabbit anti-PfRab6 antibody (see Fig. S3 in the supplemental material). Importantly, PArt overexpression did not modify its intracellular distribution pattern.

The overexpression of PArt did not result in any modifications of *in vitro* parasite development, with unchanged growth rates and length of cycle compared to that of FUP/CB wild-type parasites (Fig. 5A).

Parasite sensitivity to artesunate was analyzed in wild-type (FUP/CB) and PArt/myc-overexpressing parasites. Ring-form parasites were incubated in the presence of increasing concentrations of artesunate for 3 h, followed by thorough washing and further culture for 24 to 72 h. Spike exposure to artesunate delays the development of the parasites that survive treatment (37). This was confirmed here. At all time points, the development of both wild-type and overexpressing parasites surviving exposure to sublethal doses of artesunate was delayed compared to that of the untreated control. A typical illustration of the delay induced by incubation with artesunate is shown in Fig. 5A and B. At 24 h, untreated cultures had already developed to the schizont stage, whereas only trophozoites were observed in the treated cultures. Delayed development was evidenced at 72 h as well, with trophozoites and schizonts in the untreated cultures but only growth-delayed rings and trophozoites in the treated cultures. Artesunate-induced delay was less severe in PArt-overexpressing parasites, with more than half of the parasites having developed from

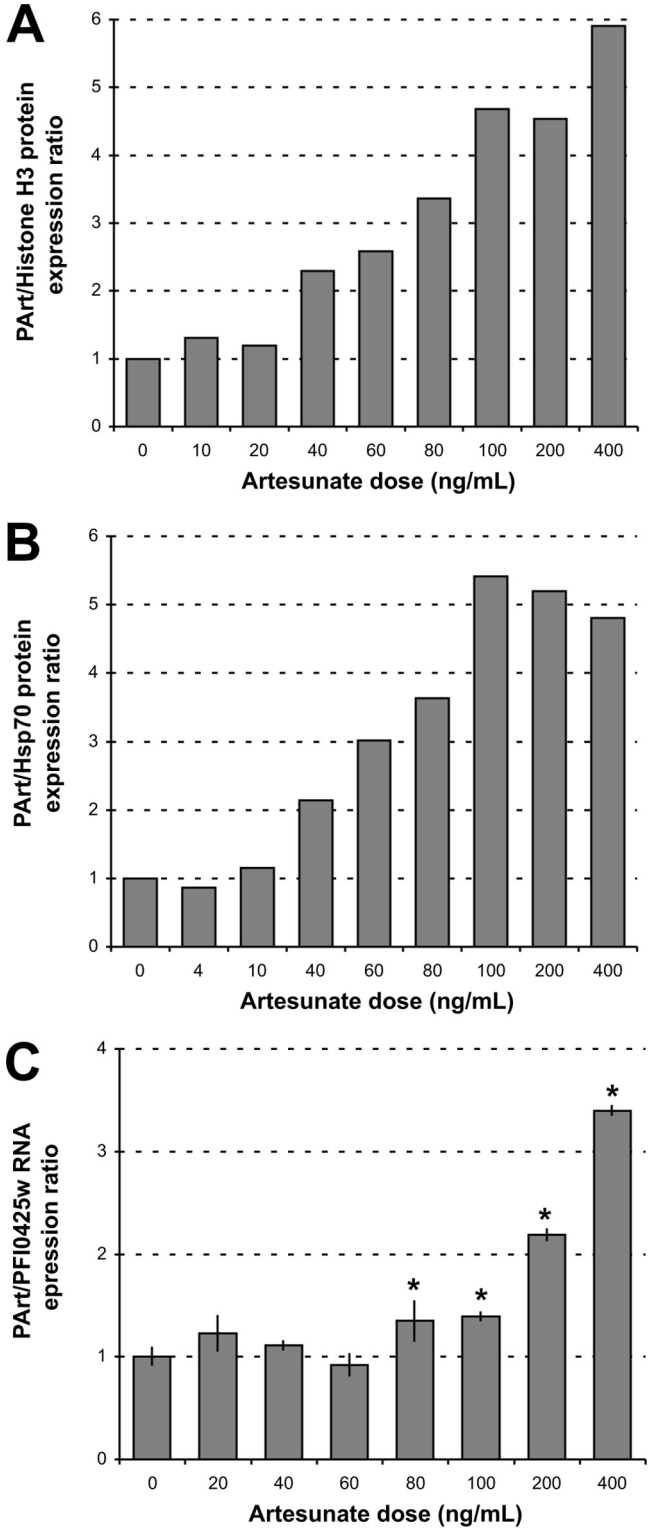

FIG. 2. Dose-dependent increase in expression of *PArt* upon drug pressure. (A) Expression ratio of PArt/histone H3 proteins measured from a Western blot of parasites exposed to increasing concentrations of artesunate for 3 h, using mouse antibodies raised against the W-rich domain of PArt. The analysis of Western blot seen in Fig. S1 in the supplemental material, using Quantity One (Bio-Rad) and histone H3 as a reference, shows a 2- to 6-fold increase of expression of PArt protein after a 3-h exposure to doses ranging from 40 to 400 ng/ml of artesunate, respectively. (B) Expression ratio of PArt/HSP70 proteins measured as described above, with PfHSP70 as the reference protein. (C) *PArt*/*PFI0425w* RNA expression ratio calculated from quantitative RT-PCR performed with parasites exposed to increasing concentrations of artesunate for 3 h. The mRNA expression level of *PArt* is normalized to the expression level of *PFI0425w*. The means from three measurements (bars indicate standard deviations) shows that a 2.2- and 3.4-fold increase of mRNA expression is observed after a 3-h exposure to 200 and 400 ng/ml of artesunate, respectively. Asterisks indicate statistical significance as determined by a one-sided Wilcoxon rank-sum test ($P = 0.05$).

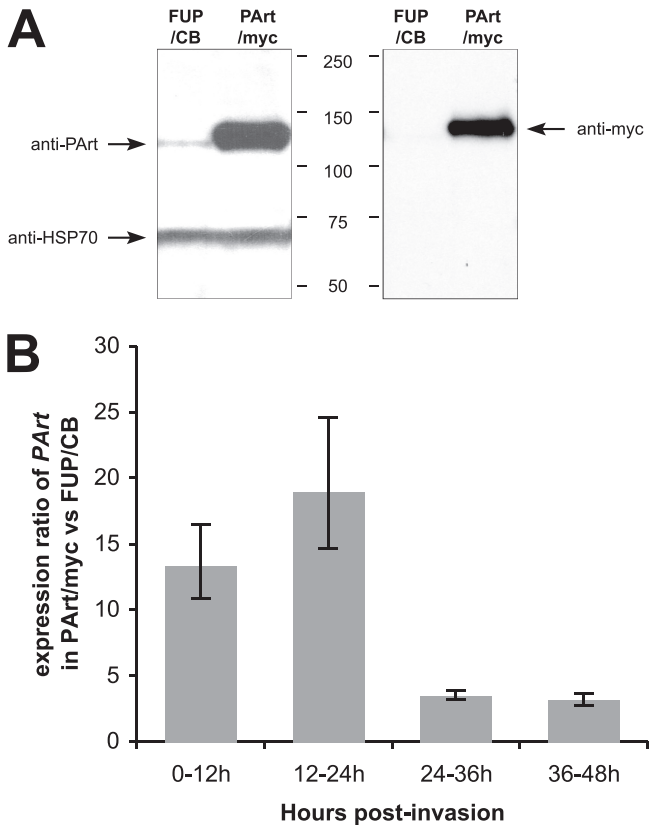

FIG. 3. Kinetics of tagged PArt expression protein during the intraerythrocytic parasite cycle. (A) Western blot analysis of the expression of PArt at the trophozoite stage (30 h postinvasion) in the wild type (FUP/CB) and in the overexpressing line (PArt/myc). Western blots were probed with mouse antibodies raised against the W-rich portion of PArt and with antibody against HSP70 as a loading control (left) or with a mouse monoclonal anti-myc antibody (right). (B) mRNA expression level of *PArt* during the development cycle of the overexpressing line PArt/myc relative to *PArt* expression in wild-type FUP/CB. An increase of RNA is observed during the first 24 h postinvasion. The expression ratio was normalized to the mRNA level of *PFI0425w*. Error bars indicate standard deviations.

rings to trophozoites when almost all parasites of the wild type were still in ring forms. As a consequence, reinvasion after treatment with sublethal doses of artesunate was not completed before the 72-h time point. Pooled results of three independent experiments show that the 72-h survival profiles at different drug concentrations were similar for FUP/CB and the transfection control line, RIF/myc parasites expressing

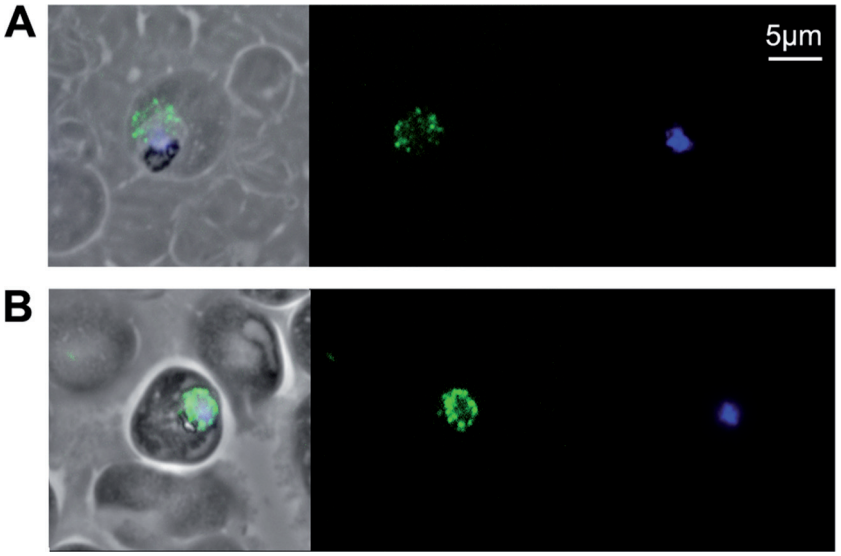

FIG. 4. Localization of PArt in FUP/CB and PArt/myc lines. Immunofluorescence assays were performed with the wild-type (FUP/CB) (A) or the overexpressing parasites (PArt/myc) (B). PArt localization with a polyclonal mouse antibody raised against the W-rich portion of the protein is shown in green. Nuclei are labeled blue with Hoescht 33342. Pictures were taken under identical exposure conditions.

myc-tagged rifin in the same vector, with an approximately 50% parasitemia decrease at 20 ng/ml compared to levels for parasites in the absence of the drug (Fig. 5C). In contrast, the survival of overexpressing parasites was 100% of that of controls without drug, although parasite development was slowed down. At 40 ng/ml survival decreased, but the overexpressing parasites survived better than the wild-type and control parasites ($P < 0.05$). A similar experiment performed with quinine (0.1 to 1 mM for 3 h) showed no effect of PArt overexpression on parasite drug susceptibility, with the overexpressing parasites being as sensitive to the drug as the controls (data not shown).

When *in vitro* chemosusceptibility was analyzed by a standard 42-h [^{3}H]hypoxanthine uptake inhibition method (6), no significant difference between FUP/CB and PArt/myc parasites could be detected with artesunate or with seven other antimalarials tested (see Table S2 in the supplemental material).

DISCUSSION

We found *PArt* (*Pf10_0026*) to be the most highly overexpressed gene in our study of the parasite transcriptome upon lethal artesunate treatment (37). This gene also was shown to be overexpressed, although to a lesser extent, under artemisinin pressure in a recent study by Hu et al. (26). The first step toward understanding the biological relevance of these observations was to show that the increase in mRNA expression was accompanied by an increased expression of the corresponding protein. The marked overexpression of *PF10_0026* detected in our transcriptome study could have reflected either a specific parasite response to overcome artesunate toxicity or more general perturbations on the path to cellular death. The data reported here indicate that the locus is part of the parasite defense mechanism against injury inflicted by the drug. The key observation was that the episome-driven overexpression of *PArt* increased the capacity to survive exposure to artesunate. High drug doses resulted in parasite death regardless of the high levels of protein expression. This indicates that PArt contributes to drug tolerance, but its protective effect is overwhelmed at high drug concentrations. As such, PArt seems to be one of several factors (including pfmdr1 [8, 44]) contributing to create the conditions for proper resistance to artemisinins, i.e., survival at high drug concentrations, to develop.

The protocol for drug exposure used to study protein expression was chosen for both our transcriptome experiments (carried out after exposure at 300 ng/ml) and to mimic the *in vivo* situation following artesunate treatment. The doses used were in the range of plasma concentrations observed *in vivo* within 3 h after drug administration (9, 38, 46), knowing that the actual levels of active drug are difficult to assess given the rapid degradation of artesunate into dihydro artemisinin both *in vivo* (36) and *in vitro* (3, 23). Under these conditions, a dose-dependent increase in PArt protein was observed under artesunate pressure. When RNA was quantified by RT-PCR under similar conditions, *PArt* RNA levels began to increase at higher doses of drug and to a lesser extent than the protein. Such quantitative and qualitative differences in parasite RNA and protein responses to artesunate may be linked to differences in detection method sensitivities to the posttranscriptional regulation of gene expression (19) and/or the protein turnover rate. Whatever the molecular mechanism underpinning the relative difference in mRNA and protein increase, the present findings indicate that levels of PArt protein increase in response to sublethal doses of artesunate.

The analysis of the W-rich domain of PArt allowed us to define a *Plasmodium*-specific gene family of 79 members, with 4 paralogs in *P. falciparum* and 39 paralogs in the *P. vivax* genome. Another family of W-rich genes of *P. falciparum* is the SURFIN family (50), but no clear homology could be detected between the W-rich regions of the two families. PArt is the only one of the four *P. falciparum* paralogs to be upregulated under artesunate pressure (37). We have, to date, no clue on

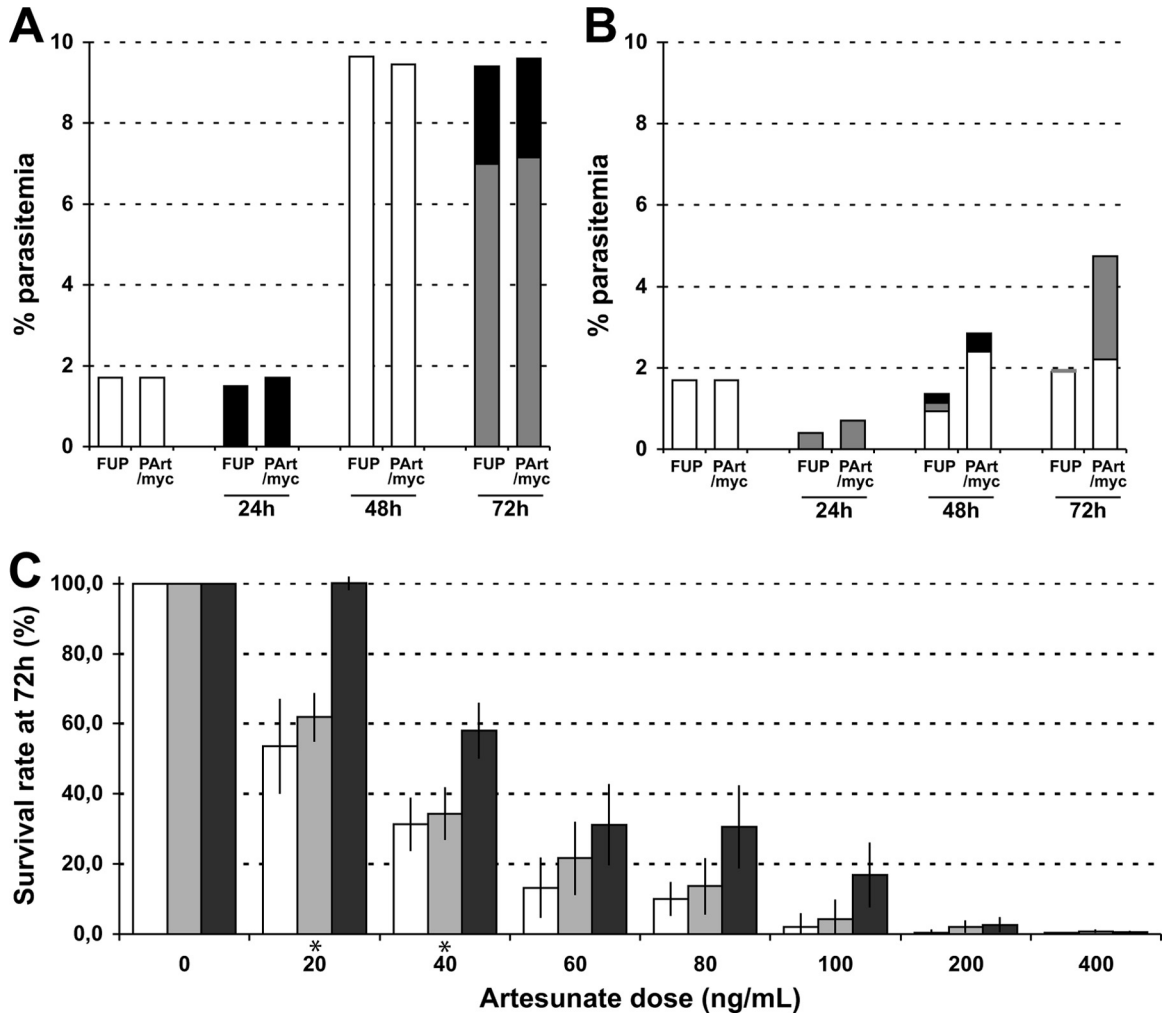

FIG. 5. Tolerance of the PArt/myc line to a 3-h exposure to artesunate. (A) Identical development of the wild type (FUP/CB) and the overexpressing transgenic line (PArt/myc) during 72 h in the absence of artesunate. Parasitemia and stage distribution were determined by the optical microscopy of Giemsa-stained blood films made every 24 h of parasite development. White bars indicate ring stages, i.e., ring-shaped parasites, uninucleated with thin cytoplasm; gray bars indicate trophozoites, i.e., uninucleated parasites with fleshy cytoplasm; black bars indicate schizonts, i.e., multinucleated parasites. (B) Artesunate induced a dose-dependent delay in the development of the wild type (FUP/CB) and the overexpressing transgenic line (PArt/myc). Parasitemia and stage distribution were determined as described above at time zero and at 24, 48, and 72 h after exposure to artesunate. Parasite reinvasion is totally completed only at 72 h due to a drug-induced delay in development. Bars are defined as described above. (C) Survival of the wild type (white bars), control transfected line (light gray bars), or overexpressed transgenic line (dark gray bars) to a 3-h incubation with increasing doses of artesunate was determined by 72 h after the end of drug exposure (pooled results from four independent experiments). The survival of drug-exposed parasites is expressed as the percentage of the parasitemia reached at 72 h in untreated cultures. A one-sided rank-sum Wilcoxon test was used to determine drug concentrations for which the survival rate of the PArt/myc line was significantly increased compared to that of controls. Doses leading to significant survival differences (20 and 40 ng/ml) are indicated by an asterisk. Error bars indicate standard deviations.

the putative function of the PArt-related protein family in the malaria parasites. Tryptophan residues have a preference for the interfacial region of lipid bilayers and thus play an important role in membrane-spanning proteins (54); the hypothetical transmembrane domain of PArt may play a role in this context. The tryptophan residues participate in protein folding in aqueous solutions, in which they contribute to maintain hydrophobic contacts (30). In the transcription factor family myb, the presence and periodicity of W is essential for DNA binding (28). Another type of domain in which W plays an essential role is the WW domain, which binds to proline residues and in which W residues are separated by 20 to 22 amino acids (5). Multiple functions have been described for these domains, including transcription regulation, protein ubiquitination, and cell cycle control (29, 45). Another frequently represented amino acid in the C-terminal region of PArt is K. The pi electron system of W results in negatively charged clouds that can participate in cation-pi interactions that occur in proteins between the negatively charged electron cloud of any aromatic residue and various cationic species, such as ions or side chains of positively charged amino acids (55). Cation-pi interactions are important in proteins for substrate binding, catalysis, and ion channel activity (7).

The multiplicity of biological functions in which W residues

play a role does not allow us to single out a given hypothesis concerning the role the overexpression of PArt plays in the increased parasite tolerance to artesunate shown in the present study. Immunofluorescence images indicate that the PArt protein is localized in the parasite cytoplasm and not in the Golgi apparatus, as shown by the use of an anti-PfRab6 antibody. The protein does not colocalize with the food vacuole, as do transporters such as *Pfcrt* or *Pfmdr1* (43). However, the fluorescence pattern could be compatible with localization in the vacuole-associated neutral lipid bodies (41) recently shown to concentrate endoperoxide derivatives of artemisinin (22). An attractive hypothesis is that PArt has a chaperone-like function or is involved in the turnover of proteins altered by the oxidative stress induced by artesunate.

The impact of PArt overexpression on susceptibility to artesunate could be best assessed 72 h after drug exposure, as parasite development was slowed down in the presence of sublethal doses of artesunate, and thus invasion was totally achieved at 72 h only, as opposed to 48 h for untreated controls. At 20 ng/ml, a dose that killed approximately 50% of the control parasites, 100% of the transgenic PArt-overexpressing parasites survived. This indicates that PArt plays a role in defense mechanisms deployed by the parasite in response to drug-induced damage rather than in events leading to parasite death.

In contrast to our transgenic parasites, a selection of parasites with reduced artemisinin susceptibility required prolonged drug exposure *in vitro* (8, 51). The artesunate-tolerant *P. falciparum* F32-ART line, recently described by Witkowski et al. (51), was obtained by stepwise, discontinuous *in vitro* selection with increasing doses of artesunate for 3 years. Chavchich et al. used a stepwise increase in artelinic acid for 28 months (8). The F32-ART parasites survived exposure to very high doses of the drug. Resistance was attributed to a small subpopulation of ring stages triggered in developmental arrest and able to persist for at least 96 h after a transient exposure to high doses of the drug, a physiological state referred to as quiescence or dormancy (25, 47, 51). The temporary quiescence of these ring stages was alleviated after drug removal, and the parasites were able to continue their development. This suggests that F32-ART tolerance to artemisinins involves the induction of quiescent forms of resistant parasites on which the drug is inactive. Although our data do not exclude the possible involvement of some dormant forms in the culture of PArt overexpressers, we show that other mechanisms come into play. Indeed, the overexpression of PArt reduced the delay in parasite development and the killing of parasites in response to a flash exposure of artesunate. As a consequence, the transgenic PArt overexpresser reached higher densities, with more mature parasites at 72 h than the control susceptible lines. The conclusion of a distinct effect in transgenic PArt-overexpressing lines compared to that in drug-induced F32-ART is supported by the absence of *PF10-0026* from the list of genes overexpressed by F32-ART described by Witkowski et al. (51). This may reflect different phenotypes: the artesunate-tolerant F32 line survived a 24-h exposure to high artemisinin concentrations (up to 9 μM), while our PArt overexpresser succumbed to doses above 1 μM, although it tolerated moderate spike doses of artesunate (100 nM).

To date, it has been difficult to detect tolerance to artesunate, as observed in the field, with an *in vitro* assay. *In vivo*, the best parasitological measure of artesunate susceptibility appears to be the determination of parasitemia at day 3 after treatment as an evaluation of parasite clearance time (14, 39). This tolerance is poorly detected by Desjardins-type resistance assays, which are designed to explore drug sensitivity based on the maturation of trophozoite and schizont parasite stages, which are the main targets of antimalarial drugs other than artemisinin derivatives (12). The early window of development represented by rings that are exquisitely sensitive to artesunate has not been investigated, leading to the poor detection of parasite tolerance to this family of antimalarials. In this line, a conventional Desjardins test poorly reflected the level of drug susceptibility of artesunate-tolerant parasites (6, 48). Indeed, such a test did not allow us to detect the artesunate tolerance of PfArt/myc parasites. This led us to devise a more adapted *in vitro* assay based on a 3-h drug exposure protocol. It would be interesting to assess how the spike exposure *in vitro* with high doses of the drug correlates with *in vivo* survival. Furthermore, the study of *PArt* in parasites isolated from patients tolerant to the artemisinin component of ACT should show whether this gene, through its expression level and the polymorphism of its promoter or coding regions, could serve as a molecular marker of tolerance to artemisinins.

ACKNOWLEDGMENTS

We are grateful to Thierry Blisnick, Anthony Bouillon, Geneviève Milon, Denise Mattei, Innocent Safeukui, Robert Ménard, Rémy Durand, and Pierre Buffet for invaluable advice and help throughout this work and to Gordon Langsley for generously providing the anti-Rab6 immune serum.

This work received financial support from the Institut Pasteur, the Centre National De la Recherche Scientifique (CNRS), the Délégation Générale pour l'Armement (DGA 22120/DSP/SREAF and 04 34 025), the Programme PAL+/Fonds National pour la Science, the Fonds Dédié "Combattre les Maladies Parasitaires" (Sanofi-Aventis/Ministère de l'Enseignement Supérieur et de la Recherche), and the BioMalPar European Network of Excellence, which was supported by a European grant and the Programme Génopole. Guillaume Deplaine was supported by grants from the Délégation Générale à l'Armement (fellowship 05 60 00 032), F. Lacoste (Fondation Ackerman-Fondation de France), and the Région Ile de France. Catherine Lavazec was supported in part by the Fonds Dédié "Combattre les Maladies Parasitaires" (Sanofi-Aventis/Ministère de l'Enseignement Supérieur et de la Recherche). Onguma Natalang was supported in part by the Thailand Research Fund through the Royal Golden Jubilee Ph.D. programme (grant no. PHD/0157/2542). Emmanuel Bischoff was supported by the Délégation Générale pour l'Armement (DGA 22120/DSP/SREAF and 04 34 025).

We declare that no competing interests exist.

REFERENCES

1. **Adams, P. A., P. A. Berman, T. J. Egan, P. J. Marsh, and J. Silver.** 1996. The iron environment in heme and heme-antimalarial complexes of pharmacological interest. J. Inorg. Biochem. **63:**69–77.
2. **Asawamahasakda, W., I. Ittarat, Y. M. Pu, H. Ziffer, and S. R. Meshnick.** 1994. Reaction of antimalarial endoperoxides with specific parasite proteins. Antimicrob. Agents Chemother. **38:**1854–1858.
3. **Batty, K. T., K. F. Ilett, T. Davis, and M. E. Davis.** 1996. Chemical stability of artesunate injection and proposal for its administration by intravenous infusion. J. Pharm. Pharmacol. **48:**22–26.
4. **Bora, H., et al.** 2011. Plasmodium vivax tryptophan-rich antigen PvTRAg33.5 contains alpha helical structure and multidomain architecture. PLoS One **6:**e16294.
5. **Bork, P., and M. Sudol.** 1994. The WW domain: a signalling site in dystrophin? Trends Biochem. Sci. **19:**531–533.
6. **Briolant, S., et al.** 2010. Absence of association between piperaquine in vitro responses and polymorphisms in the pfcrt, pfmdr1, pfmrp, and pfnhe genes in Plasmodium falciparum. Antimicrob. Agents Chemother. **54:**3537–3544.

7. **Chan, D. I., E. J. Prenner, and H. J. Vogel.** 2006. Tryptophan- and arginine-rich antimicrobial peptides: structures and mechanisms of action. Biochim. Biophys. Acta **1758:**1184–1202.
8. **Chavchich, M., et al.** 2010. Role of pfmdr1 amplification and expression in induction of resistance to artemisinin derivatives in Plasmodium falciparum. Antimicrob. Agents Chemother. **54:**2455–2464.
9. **Crabb, B. S., T. Triglia, J. G. Waterkeyn, and A. F. Cowman.** 1997. Stable transgene expression in Plasmodium falciparum. Mol. Biochem. Parasitol. **90:**131–144.
10. **de Castro, F. A., et al.** 1996. Identification of a family of Rab G-proteins in Plasmodium falciparum and a detailed characterisation of pfrab6. Mol. Biochem. Parasitol. **80:**77–88.
11. **Deitsch, K., C. Driskill, and T. Wellems.** 2001. Transformation of malaria parasites by the spontaneous uptake and expression of DNA from human erythrocytes. Nucleic Acids Res. **29:**850–853.
12. **Desjardins, R. E., C. J. Canfield, J. D. Haynes, and J. D. Chulay.** 1979. Quantitative assessment of antimalarial activity in vitro by a semiautomated microdilution technique. Antimicrob. Agents Chemother. **16:**710–718.
13. **Ding, X. C., H. P. Beck, and G. Raso.** 2011. Plasmodium sensitivity to artemisinins: magic bullets hit elusive targets. Trends Parasitol. **27:**73–81.
14. **Dondorp, A. M., et al.** 2009. Artemisinin resistance in Plasmodium falciparum malaria. N. Engl. J. Med. **361:**455–467.
15. **Dondorp, A. M., et al.** 2010. Artemisinin resistance: current status and scenarios for containment. Nat. Rev. Microbiol. **8:**272–280.
16. **Duraisingh, M. T., T. Triglia, and A. F. Cowman.** 2002. Negative selection of Plasmodium falciparum reveals targeted gene deletion by double crossover recombination. Int. J. Parasitol. **32:**81–89.
17. **Eckstein-Ludwig, U., et al.** 2003. Artemisinins target the SERCA of Plasmodium falciparum. Nature **424:**957–961.
18. **Fandeur, T., S. Bonnefoy, and O. Mercereau-Puijalon.** 1991. In vivo and in vitro derived Palo Alto lines of Plasmodium falciparum are genetically unrelated. Mol. Biochem. Parasitol. **47:**167–178.
19. **Foth, B. J., N. Zhang, S. Mok, P. R. Preiser, and Z. Bozdech.** 2008. Quantitative protein expression profiling reveals extensive post-transcriptional regulation and post-translational modifications in schizont-stage malaria parasites. Genome Biol. **9:**R177.
20. **Ginsburg, H., S. Kutner, M. Krugliak, and Z. I. Cabantchik.** 1985. Characterization of permeation pathways appearing in the host membrane of Plasmodium falciparum infected red blood cells. Mol. Biochem. Parasitol. **14:**313–322.
21. **Golenser, J., J. H. Waknine, M. Krugliak, N. H. Hunt, and G. E. Grau.** 2006. Current perspectives on the mechanism of action of artemisinins. Int. J. Parasitol. **36:**1427–1441.
22. **Hartwig, C. L., et al.** 2009. Accumulation of artemisinin trioxane derivatives within neutral lipids of Plasmodium falciparum malaria parasites is endoperoxide-dependent. Biochem. Pharmacol. **77:**322–336.
23. **Haynes, R. K.** 2006. From artemisinin to new artemisinin antimalarials: biosynthesis, extraction, old and new derivatives, stereochemistry and medicinal chemistry requirements. Curr. Top. Med. Chem. **6:**509–537.
24. **Haynes, R. K., et al.** 2007. Artesunate and dihydroartemisinin (DHA): unusual decomposition products formed under mild conditions and comments on the fitness of DHA as an antimalarial drug. ChemMedChem **2:**1448–1463.
25. **Hoshen, M. B., K. Na-Bangchang, W. D. Stein, and H. Ginsburg.** 2000. Mathematical modelling of the chemotherapy of Plasmodium falciparum malaria with artesunate: postulation of "dormancy", a partial cytostatic effect of the drug, and its implication for treatment regimens. Parasitology **121:**237–246.
26. **Hu, G., et al.** 2010. Transcriptional profiling of growth perturbations of the human malaria parasite Plasmodium falciparum. Nat. Biotechnol. **28:**91–98.
27. **Jambou, R., et al.** 2005. Resistance of Plasmodium falciparum field isolates to in-vitro artemether and point mutations of the SERCA-type PfATPase6. Lancet **366:**1960–1963.
28. **Kanei-Ishii, C., et al.** 1990. The tryptophan cluster: a hypothetical structure of the DNA-binding domain of the myb protooncogene product. J. Biol. Chem. **265:**19990–19995.
29. **Kay, B. K., M. P. Williamson, and M. Sudol.** 2000. The importance of being proline: the interaction of proline-rich motifs in signaling proteins with their cognate domains. FASEB J. **14:**231–241.
30. **Klein-Seetharaman, J., et al.** 2002. Long-range interactions within a non native protein. Science **295:**1719–1722.
31. **Krishna, S., L. Bustamante, R. K. Haynes, and H. M. Staines.** 2008. Artemisinins: their growing importance in medicine. Trends Pharmacol. Sci. **29:**520–527.
32. **Krishna, S., S. Pulcini, F. Fatih, and H. Staines.** 2010. Artemisinins and the biological basis for the PfATP6/SERCA hypothesis. Trends Parasitol. **26:**517–523.
33. **Krishna, S., C. J. Woodrow, H. M. Staines, R. K. Haynes, and O. Mercereau-Puijalon.** 2006. Re-evaluation of how artemisinins work in light of emerging evidence of in vitro resistance. Trends Mol. Med. **12:**200–205.
34. **Lavazec, C., S. Sanyal, and T. J. Templeton.** 2006. Hypervariability within the Rifin, Stevor and Pfmc-2TM superfamilies in Plasmodium falciparum. Nucleic Acids Res. **34:**6696–6707.
35. **Maude, R. J., et al.** 2009. The last man standing is the most resistant: eliminating artemisinin-resistant malaria in Cambodia. Malar. J. **8:**31.
36. **Medhi, B., S. Patyar, R. S. Rao, D. S. P. Byrav, and A. Prakash.** 2009. Pharmacokinetic and toxicological profile of artemisinin compounds: an update. Pharmacology **84:**323–332.
37. **Natalang, O., et al.** 2008. Dynamic RNA profiling in Plasmodium falciparum synchronized blood stages exposed to lethal doses of artesunate. BMC Genomics **9:**388.
38. **Newton, P. N., et al.** 2006. The pharmacokinetics of intravenous artesunate in adults with severe falciparum malaria. Eur. J. Clin. Pharmacol. **62:**1003–1009.
39. **Noedl, H., D. Socheat, and W. Satimai.** 2009. Artemisinin-resistant malaria in Asia. N. Engl. J. Med. **361:**540–541.
40. **Ntumngia, F. B., N. Bahamontes-Rosa, and J. F. Kun.** 2005. Genes coding for tryptophan-rich proteins are transcribed throughout the asexual cycle of Plasmodium falciparum. Parasitol. Res. **96:**347–353.
41. **Palacpac, N. M., Y. Hiramine, F. Mi-ichi, et al.** 2004. Developmental-stage-specific triacylglycerol biosynthesis, degradation and trafficking as lipid bodies in Plasmodium falciparum-infected erythrocytes. J. Cell Sci. **117:**1469–1480.
42. **Pasvol, G., R. J. Wilson, M. E. Smalley, and J. Brown.** 1978. Separation of viable schizont-infected red cells of Plasmodium falciparum from human blood. Ann. Trop. Med. Parasitol. **72:**87–88.
43. **Sanchez, C. P., A. Dave, W. D. Stein, and M. Lanzer.** 2010. Transporters as mediators of drug resistance in Plasmodium falciparum. Int. J. Parasitol. **40:**1109–1118.
44. **Sidhu, A. B., et al.** 2006. Decreasing pfmdr1 copy number in plasmodium falciparum malaria heightens susceptibility to mefloquine, lumefantrine, halofantrine, quinine, and artemisinin. J. Infect. Dis. **194:**528–535.
45. **Sudol, M., and T. Hunter.** 2000. NeW wrinkles for an old domain. Cell **103:**1001–1004.
46. **Teja-Isavadharm, P., et al.** 1996. Comparative bioavailability of oral, rectal, and intramuscular artemether in healthy subjects: use of simultaneous measurement by high performance liquid chromatography and bioassay. Br. J. Clin. Pharmacol. **42:**599–604.
47. **Teuscher, F., et al.** 2010. Artemisinin-induced dormancy in plasmodium falciparum: duration, recovery rates, and implications in treatment failure. J. Infect. Dis. **202:**1362–1368.
48. **Trager, W., and J. B. Jensen.** 1976. Human malaria parasites in continuous culture. Science **193:**673–675.
49. **Wang, J., et al.** 2010. Artemisinin directly targets malarial mitochondria through its specific mitochondrial activation. PLoS One **5:**e9582.
50. **Winter, G., et al.** 2005. SURFIN is a polymorphic antigen expressed on Plasmodium falciparum merozoites and infected erythrocytes. J. Exp. Med. **201:**1853–1863.
51. **Witkowski, B., et al.** 2010. Increased tolerance to artemisinin in Plasmodium falciparum is mediated by a quiescence mechanism. Antimicrob. Agents Chemother. **54:**1872–1877.
52. **Wu, Y., C. D. Sifri, H. H. Lei, X. Z. Su, and T. E. Wellems.** 1995. Transfection of Plasmodium falciparum within human red blood cells. Proc. Natl. Acad. Sci. U. S. A. **92:**973–977.
53. **Yang, H., et al.** 2003. Changes in susceptibility of Plasmodium falciparum to artesunate in vitro in Yunnan Province, China. Trans. R. Soc. Trop. Med. Hyg. **97:**226–228.
54. **Yau, W. M., W. C. Wimley, K. Gawrisch, and S. H. White.** 1998. The preference of tryptophan for membrane interfaces. Biochemistry **37:**14713–14718.
55. **Zacharias, N., and D. A. Dougherty.** 2002. Cation-pi interactions in ligand recognition and catalysis. Trends Pharmacol. Sci. **23:**281–287.